XVII IMEKO World Congress
Metrology in the 3rd Millennium
June 22–27, 2003, Dubrovnik, Croatia

Interaction between ultrasound and streaming fluid in vortex shedding flow metering

Christian Filips, Volker H. Hans

Institute of Measurement and Control, University Duisburg-Essen, Schuetzenbahn 70, 45117 Essen, Germany

Abstract – In the past in vortex-shedding flow meters pressure sensors in combination with big bluff bodies have been used. In the last few years the dimension of bluff bodies were reduced using ultrasound sensors due to higher sensibility [1]. The frequency of periodically generated vortices are directly connected to the flow velocity. The signals are modulated in amplitude as well as in phase. The information are in the sidebands of the ultrasonic signal. Different carrier frequencies in combination with different dimensions of bluff bodies are examined.

Keywords: vortex-shedding flow metering, ultrasonic carrier frequency, bluff body.

1. INTRODUCTION

Since many years vortex-shedding flow metering is an efficient flow measuring method. The use of big bluff bodies leads to high losses of pressure in streaming fluid. In general the size of bluff body height was recommended as 24% of pipe's cross-section [2] for the detection of vortices by pressure sensors.

Using ultrasonic signals it could be shown [1] that the bluff body size could be reduced drastically.

2. FUNDAMENTALS

The generated vortices modulate the ultrasound waves transmitted through the flow periodically. The influence of amplitude and phase results in complex modulation. Vortices are disturbances in the flow with a varying density and pressure field. The modulation of phase depends on local changes of density which lead to changes in speed of sound. The effects of the amplitude modulation are caused by absorption and diffraction of sound.

2.1. Signal processing

Due to the superposition of both components it is impossible to determine each modulation component directly from the modulated signal. The signal consists of a real and an imaginary component. By undersampling with integer multiples of the carrier frequency which does not contain any information the carrier frequency can be shifted to zero in the frequency domain. This principle is illustrated by a rotating pointer in the complex area which is stopped by undersampling (fig. 1) [3].

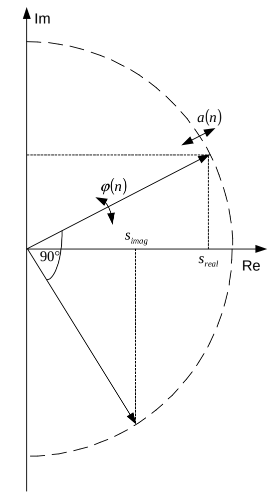

Fig. 1. Principle of complex bandpass sampling

Due to modulation the pointer changes in amplitude and in phase. Only real magnitudes can be measured. However, the imaginary part can be evaluated by a $90°$ shifted pointer which corresponds to the imaginary magnitude illustrated on the real axis. The relationship between the real and imaginary part is described by Hilbert-Transformation. The performance of Hilbert-Transformation is realised by sampling two points shifted by $90°$ [3].

2.2. Different carrier frequencies

The characteristic of ultrasonic signals depends on the interaction of generated structures and ultrasound. The influence of different carrier frequencies is directly connected to different wavelengths. The resolution of structures depends on the wavelength of the carrier frequency. The following carrier frequencies have been examined:

- $80kHz$,
- $160kHz$,
- $220kHz$.

2.3. Determining flow velocity

Bluff bodies inside a pipe generate vortices. The vortex frequency depends on the flow velocity. This coherence is given by the Strouhal-Number

$$Sr = \frac{d \cdot f_V}{u_m}, \quad (1)$$

where d is the diameter of the bluff body, f_V the vortex frequency and u_m the average velocity. The vortex frequency is in the range from some Hz to about $3kHz$ which depends on the dimension of bluff body and the actual flow velocity. Vortex structures separate alternately from the edges. The one-sided vortex sequence corresponds to the vortex frequency. The vortex sequence on the opposite edge is shifted by a half period time and also corresponds to the vortex frequency. Due to the high sensitivity ultrasound detects all generated vortices which cause the double vortex frequency called modulation frequency.

3. RESULTS

Usually triangular shapes of bluff bodies are applied for vortex generation [2]. Varying shapes lead to interesting new aspects of the arrangement of bluff bodies, vortex frequencies and pressure losses behind the bluff bodies. In the following the unusual shape of threaded control rod will be presented.

The following results consider the influence of different carrier frequencies using different dimensions of threaded control rods as bluff bodies. Considering both modulation components the evaluation of the results are illustrated in two chapters with low and high flow velocities.

3.1. The demodulated amplitude

An overview about the interaction of generated structures and different carrier frequencies is shown in fig. 2 for a low velocity at $2m/s$ by evaluating the demodulated amplitude using a M4 bluff body.

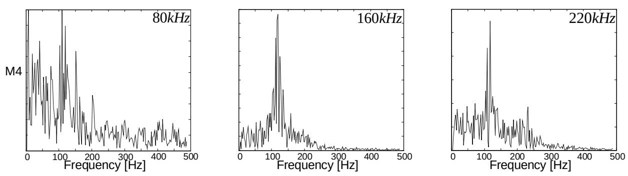

Fig. 2. Evaluation of demodulated amplitude for different ultrasound carrier frequencies at $2m/s$ using M4

The wavelength of the carrier frequency is responsible for different influences. With increasing carrier frequency the wavelength decreases. Modulation effects in streaming flow which are lower than the wavelength of the carrier frequency aren't recognized and don't appear in the signal. Periodical vortex shedding of a M4 threaded control rod shows a wavelength of about $\lambda_{M4} = 16{,}7mm$. The lowest carrier frequency of $80kHz$ corresponds to a wavelength of about $\lambda_{80} = 4{,}3mm$. The vortices could be determined but due to the higher energy of the flow in the spectrum lower frequencies dominate and modulate the ultrasonic signal. Using higher carrier frequencies the vortex frequency could be clearly determined without any influence of disturbances.

With increasing bluff body size to M10 the sensitivity of bluff body is reduced (fig. 3).

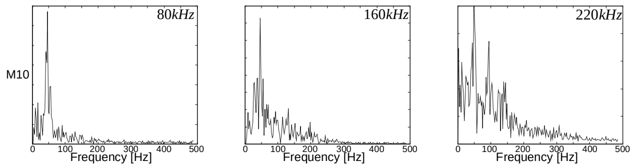

Fig. 3. Evaluation of demodulated amplitude for different ultrasound carrier frequencies at $2m/s$ using M10

The highest carrier frequency of $220kHz$ shows the effect mentioned above. Due to the higher energy of the vortices the signal is modulated as well with vortex as with modulation frequency. In the evaluation the vortex frequency dominates in the spectrum.

Using M20 the biggest bluff body the results are similar to evaluation of M10 (fig. 4). All carrier frequencies detect the vortex frequency, but using $80kHz$ the results are more clear and not overlapped with noise.

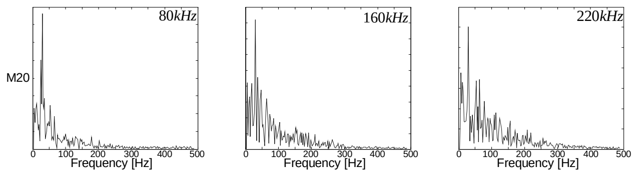

Fig. 4. Evaluation of demodulated amplitude for different ultrasound carrier frequencies at $2m/s$ using M20

The vortices are recognized due to influence of structures with high wavelength. The following figures show the results using a high velocity of $25m/s$.

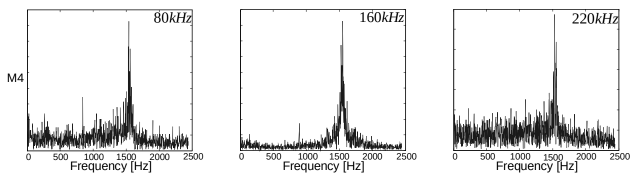

Fig. 5. Evaluation of demodulated amplitude for different ultrasound carrier frequencies at $25m/s$ using M4

Figure 5 shows the results of M4. Even in this case the vortex frequency is detected. A carrier frequency of $160kHz$ leads to clear and stable results.

The high velocity in combination with bigger bluff bodies increases the noise. The examination of M10 leads to different results (fig. 6). The low carrier frequency detects the vortex frequency of $575Hz$. Using $160kHz$ three peaks are shown in the spectrum and the modulation frequency of $1150Hz$ dominates. The high carrier frequency of $220kHz$ is modulated by the modulation frequency. The vortex frequency can't be detected.

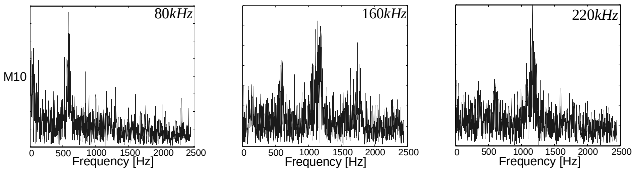

Fig. 6. Evaluation of demodulated amplitude for different ultrasound carrier frequencies at $25m/s$ using M10

Similar results are evaluated using M20 (fig. 7).

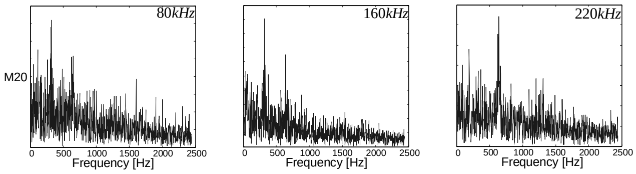

Fig. 7. Evaluation of demodulated amplitude for different ultrasound carrier frequencies at $25m/s$ using M20

With increasing velocity and increasing size of bluff body low carrier frequencies detect the vortex frequency. Using bigger bluff bodies the vortex sequence decreases and with higher carrier frequency the modulation frequency dominates in the signal.

3.2. The demodulated phase

Analogous to the demodulated amplitude the following illustrations show an overview about the demodulated phase considering different carrier frequencies and bluff body sizes. The examination is executed in the same order as done before.

The phase demodulation is limited by arctan-function in the range between $-180° \le \varphi \le 180°$. Comparing M4 threaded control rod in figure 8 with figure 2 nearly the same behaviour is shown. The result in figure 8 shows also that the evaluation of phase leads to more stable results with higher content of information and less noise.

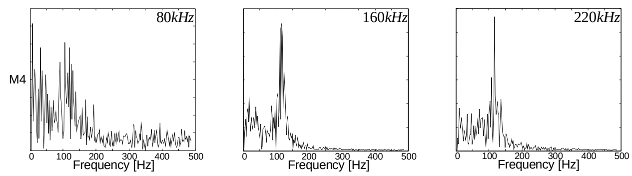

Fig. 8. Evaluation of demodulated phase for different ultrasound carrier frequencies at $2m/s$ using M4

The vortices which are generated by using a M10 bluff body are clearly detected by each carrier frequency (fig. 9).

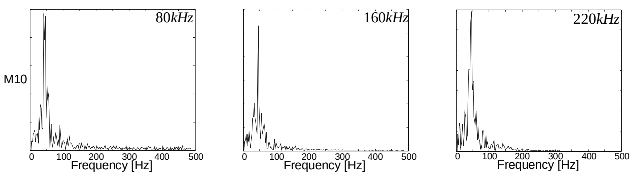

Fig. 9. Evaluation of demodulated phase for different ultrasound carrier frequencies at $2m/s$ using M10

In comparison with figure 3 the higher carrier frequencies aren't influenced in that kind by stochastic structures by using phase information.

The same explanation could be given using M20 (fig. 10).

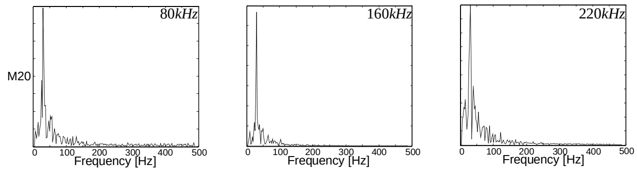

Fig. 10. Evaluation of demodulated phase for different ultrasound carrier frequencies at $2m/s$ using M20

With increasing flow velocity up to $25m/s$ the results of the examinations are shown in the following figures.

Even in this case using M4 the vortex frequency is detected by each carrier frequency (fig. 11).

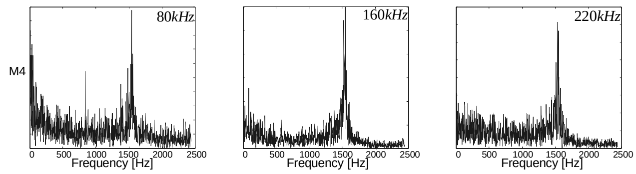

Fig. 11. Evaluation of demodulated phase for different ultrasound carrier frequencies at $25m/s$ using M4

A clear result represents the carrier frequency of $160kHz$.

Increasing the bluff body size the carrier frequency of $220kHz$ doesn't detect a characteristic frequency of M10 (fig. 12).

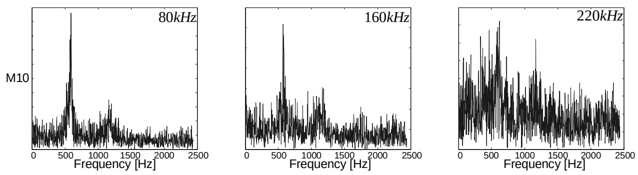

Fig. 12. Evaluation of demodulated phase for different ultrasound carrier frequencies at $25m/s$ using M10

The modulation intensity and the stochastic influence is too high which leads to errors in the evaluation.

Also by using M20 the higher carrier frequencies aren't able to detect a dominant frequency (fig. 13). Best results are shown by using $80kHz$.

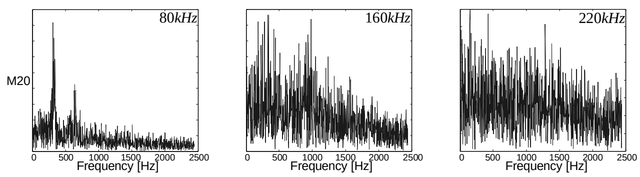

Fig. 13. Evaluation of demodulated phase for different ultrasound carrier frequencies at $25m/s$ using M20

Low carrier frequencies aren't influenced by stochastic structures in the flow. This leads to an exact evaluation of the vortex frequency. The wavelength of the structure isn't recognized by low carrier frequencies. This example shows that with increasing size of bluff body the carrier frequency must be reduced. Despite of transcending the defined range good results can be obtained for high modulation intensities and low carrier frequencies. Carrier frequency and size of bluff body must be co-ordinated.

3. CONCLUSION

It is obvious that further signal analysis is related to the evaluation of phase. It can be seen that even very small bluff body sizes generate vortices of high frequencies resulting in distinct peaks in the frequency domain. High carrier frequencies lead to better results than lower frequencies in combination with small bluff bodies.

REFERENCES

[1] H. Windorfer, "Optimierung von Wirbelfrequenzmeßgeräten mit demodulierten Ultraschallsignalen", PhD thesis, University of Essen, Shaker Verlag, 2001.

[2] R. C. Baker, "Flow measurement handbook", Cambridge Univ. Press, 2000.

[3] V. Skwarek, "An improved method for hardware based complex demodulation", Measurement 29/2, 87-93, 2001.

Author: Dipl.-Ing. Christian Filips, Prof. Dr.-Ing. Volker H. Hans, University Duisburg-Essen, Institute of Measurement and Control, Schuetzenbahn 70, 45117 Essen, Germany, Phone: +49-201-1832898, Fax: +49-201-183932898, Email: christian.filips@uni-essen.de